

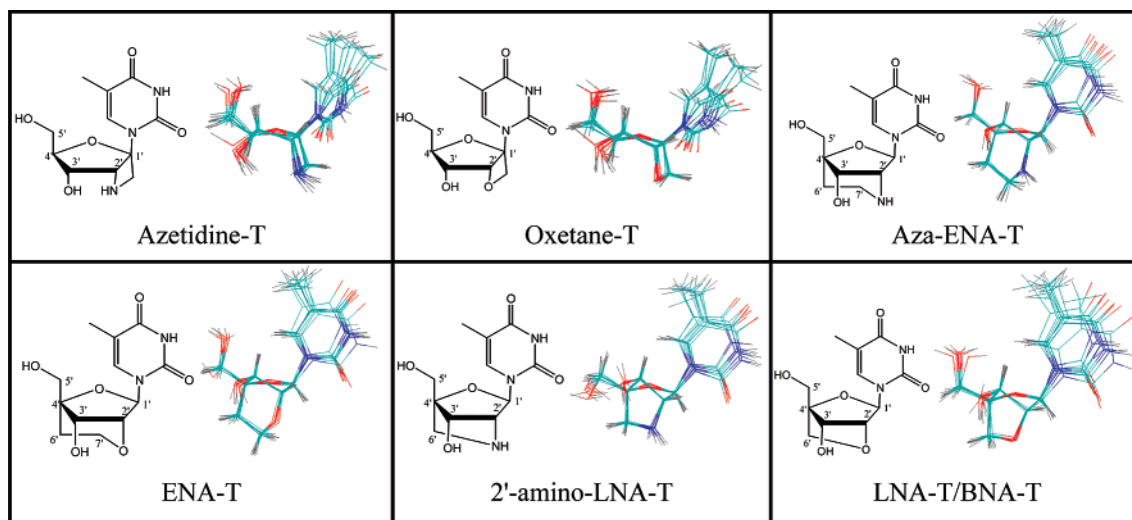
Chemical and Structural Implications of 1',2'- versus 2',4'-Conformational Constraints in the Sugar Moiety of Modified Thymine Nucleosides

Oleksandr Plashkevych,* Subhrangsu Chatterjee, Dmytro Honcharenko, Wimal Pathmasiri, and Jyoti Chattopadhyaya*

Department of Bioorganic Chemistry, Box 581, Biomedical Center, Uppsala University, SE-75123 Uppsala, Sweden

oleksandr@boc.uu.se; jyoti@boc.uu.se

Received February 21, 2007



In order to understand how the chemical nature of the conformational constraint of the sugar moiety in ON/RNA(DNA) dictates the duplex structure and reactivity, we have determined molecular structures and dynamics of the conformationally constrained 1',2'-azetidine- and 1',2'-oxetane-fused thymidines, as well as their 2',4'-fused thymine (T) counterparts such as LNA-T, 2'-amino LNA-T, ENA-T, and aza-ENA-T by NMR, *ab initio* (HF/6-31G** and B3LYP/6-31++G**), and molecular dynamics simulations (2 ns in the explicit aqueous medium). It has been found that, depending upon whether the modification leads to a bicyclic 1',2'-fused or a tricyclic 2',4'-fused system, they fall into two distinct categories characterized by their respective internal dynamics of the glycosidic and the backbone torsions as well as by characteristic *North-East* type sugar conformation ($P = 37^\circ \pm 27^\circ$, $\phi_m = 25^\circ \pm 18^\circ$) of the 1',2'-fused systems, and (ii) pure *North* type ($P = 19^\circ \pm 8^\circ$, $\phi_m = 48^\circ \pm 4^\circ$) for the 2',4'-fused nucleosides. Each group has different conformational hyperspace accessible, despite the overall similarity of the *North*-type conformational constraints imposed by the 1',2'- or 2',4'-linked modification. The comparison of pK_a s of the 1-thyminylyl aglycon as well as that of endocyclic sugar-nitrogen obtained by theoretical and experimental measurements showed that the nature of the sugar conformational constraints steer the physicochemical property (pK_a) of the constituent 1-thyminylyl moiety, which in turn can play a part in tuning the strength of hydrogen bonding in the basepairing.

Introduction

Chemical modifications of the sugar moiety of oligonucleotides (ON) have shown its enormous potential to achieve the

sequence-specific control of gene expression by improving ON's stability to cellular nucleases and binding to target RNA or DNA with high specificity, thereby enhancing the overall efficiency of the ON as an antisense, antigene, or RNAi agent.¹⁻⁵ Sugar

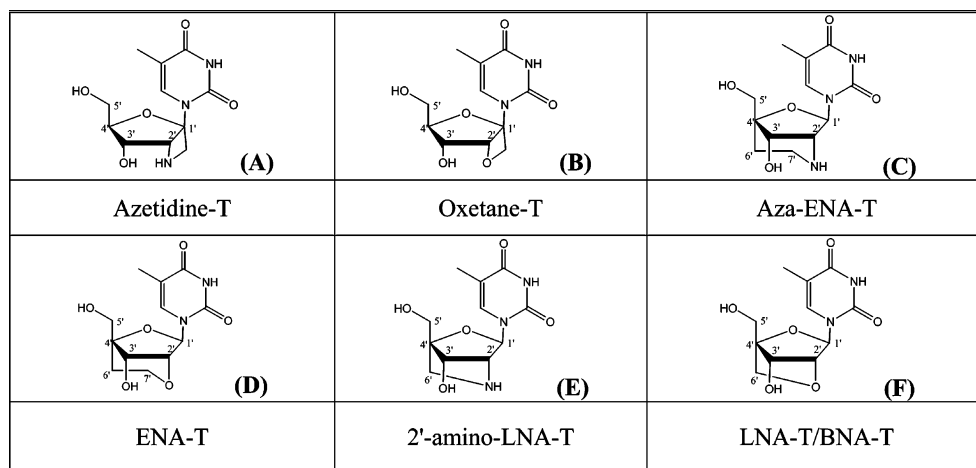


FIGURE 1. Molecular structures of (A) the 1',2'-azetidine-⁹ and (B) the -oxetane^{10,11} fused thymidines as well as of the 2'-O,4'-C-methylene bridged nucleoside (LNA-T¹²/BNA-T¹³) (F), 2'-amino-LNA-T^{14,15} (E), ENA-T¹⁶ (D), and aza-ENA-T¹⁷ (C).

conformationally constrained oligonucleotides constitute a subclass of its own^{1,2,6-8} offering a powerful handle to dictate the stability of the homo/heteroduplex or triplex by restricting the sugar pucker to a desired conformation.

Here we report a comparison of molecular structures and dynamics of the conformationally constrained 1-thymine nucleosides bearing (a) fused four-membered 1',2'-azetidine and 1',2'-oxetane modifications⁹⁻¹¹ (azetidine-T and oxetane-T, structures A and B in Figure 1, respectively), (b) five-membered 2'-N,4'-C-methylene bridge locked nucleic acid (2'-amino-LNA-T,^{14,15} E in Figure 1) and 2'-O,4'-C-methylene bridge (LNA-T/BNA-T,^{12,13} F in Figure 1), and (c) six-membered 2'-N,4'-C-ethylene bridge (aza-ENA-T,¹⁷ C in Figure 1) and 2'-O,4'-C-ethylene bridge (ENA-T,^{16,18} D in Figure 1). The study has been performed using experimental NMR data and results of ab initio (HF/6-31G** and B3LYP/6-31++G**) and molecular

dynamics (MD) simulations (the latter employing explicit aqueous medium and 2 ns simulation time).

Earlier enzymatic and kinetic studies^{9-11,17,19,20} have reported mixed results regarding improvements in antisense properties and target affinity (thermal stability) of duplexes and triplexes containing the North type conformationally constrained 1',2'-sugar fused oligonucleotides.⁹⁻¹¹ Thus, the introduction of the 1',2'-oxetane-,^{10,11} and 1',2'-azetidine-modified⁹ pyrimidine and purine nucleotides into antisense oligonucleotides (AON)/RNA duplexes have shown sequence-specific target affinity. Compared to the native counterpart, the T_m for the AON/RNA duplexes drops by ~ -5 °C for each oxetane-T, ~ -3 °C for each oxetane-C¹¹, -4 °C for azetidine-T/U, and to -2 °C for azetidine-C⁹ incorporation in the modified AONs. No T_m drop has however been observed for the oxetane-A and oxetane-G¹⁰ modifications in the AONs.

Incorporation of the five- and six-membered 2',4'-bridged ENA-T,^{16,18} LNA-T/BNA-T,^{12,13} and their 2'-N analogues (aza-ENA-T¹⁷ and 2'-amino-LNA-T^{14,15}) into DNA or RNA strand showed, compared to the native, improved target affinity toward complementary RNA and DNA. AONs containing ENA-T and aza-ENA-T¹⁷ have shown an increase of thermal stability of the AON/RNA duplexes by $+3.5$ to $+5.2$ °C per modification which is as high as that of the isosequential LNA-T⁸ ($\Delta T_m = T_m(\text{modified}) - T_m(\text{native})$, $\Delta T_m \sim +3.5$ to $+5.2$ °C per modification) and 2'-amino-LNA-T^{14,15} ($\Delta T_m \sim +6$ to $+8$ °C per modification). Toward complementary DNA,¹² the AONs containing 2'-O,4'-C-ethylene- and 2'-N,4'-C-ethylene-bridged thymidines exhibited a moderate increase of $+3$ to $+5$ °C per modification.

Generally, the 2',4'-LNA/ENA-type modifications seem to show systematic increase in the thermal stability of AON/RNA and AON/RNA duplexes and triplexes and decrease in the AON/DNA stability.^{8,15,21,22} However, the total effect of the chemical

(1) Zamaratski, E.; Pradeepkumar, P. I.; Chattopadhyaya, J. *J. Biochem. Biophys. Methods* **2001**, *48*, 189–208.

(2) Manoharan, M. *Antisense Nucleic Acid Drug Dev.* **2002**, *12*, 103–128.

(3) Herdewijn, P. *Biochim. Biophys. Acta* **1999**, *1489*, 167–179.

(4) Kurreck, J.; Wyszko, E.; Gillen, C.; Erdmann, V. A. *Nucl. Acids Res.* **2002**, *30* (9), 1911–1918.

(5) Koizumi, M. *Biol. Pharm. Bull.* **2004**, *27* (4), 453–456.

(6) Meldgaard, M.; Wengel, J. *J. Chem. Soc., Perkin Trans. 1* **2000**, 3539–3554.

(7) Takagi, M.; Morita, K.; Nakai, D.; Nakagomi, R.; Tokui, T.; Koizumi, M. *Biochemistry* **2004**, *43* (15), 4501–4510.

(8) Morita, K.; Yamate, K.; Kurakata, S.; Abe, K.; Imanishi, T.; Koizumi, M. *Nucleic Acids Symp. Ser.* **2002**, *2* (1), 99–100.

(9) Honcharenko, D.; Varghese, O. P.; Plashkevych, O.; Barman, J.; Chattopadhyaya, J. *J. Org. Chem.* **2006**, *71*, 299–314.

(10) Pradeepkumar, P. I.; Cheruku, P.; Plashkevych, O.; Acharya, P.; Gohil, S.; Chattopadhyaya, J. *J. Am. Chem. Soc.* **2004**, *126*, 11484–11489.

(11) Pradeepkumar, P. I.; Zamaratski, E.; Foldesi, A.; Chattopadhyaya, J. *J. Chem. Soc., Perkin Trans.* **2001**, *2*, 402–408.

(12) Koshkin, A. A.; Singh, S. K.; Nielson, P.; Rajwanshi, V. K.; Kumar R.; Meldgaard, M.; Wengel, J. *Tetrahedron* **1998**, *54*, 3607–3630.

(13) Obika, S.; Nanbu, D.; Hari, Y.; Morio, K.-I.; In, Y.; Ishida, T.; Imanishi, T. *Tetrahedron Lett.* **1997**, *38* (50), 8735–8738.

(14) Singh, S. K.; Kumar, R.; Wengel, J. *J. Org. Chem.* **1998**, *63* (26), 10035–10039.

(15) Singh, S. K.; Kumar, R.; Wengel, J. *J. Org. Chem.* **1998**, *63* (18), 6078–6079.

(16) Morita, K.; Takagi, M.; Hasegawa, C.; Kaneko, M.; Tsutsumi, S.; Sone, J.; Ishikawa, T.; Imanishi, T.; Koizumi, M. *Bioorg. Med. Chem.* **2003**, *11*, 2211–2226.

(17) Varghese, O. P.; Barman, J.; Pathmasiri, W.; Plashkevych, O.; Honcharenko, D.; Chattopadhyaya, J. *J. Am. Chem. Soc.* **2006**, *128* (47), 15173–15187.

(18) Morita, K.; Yamate, K.; Kurakata, S.-I.; Watanabe, K.; Imanishi, T.; Koizumi, M. *Nucleosides, Nucleotides Nucleic Acids* **2003**, *22*, 1619.

(19) Amirkhanov, N. V.; Pradeepkumar, P. I.; Chattopadhyaya, J. *J. Chem. Soc., Perkin Trans.* **2002**, *2*, 976–984.

(20) Pradeepkumar, P. I.; Amirkhanov, N. V.; Chattopadhyaya, J. *Org. Biomol. Chem.* **2003**, *1*, 81–92.

(21) Morita, K.; Hasegawa, C.; Kaneko, M.; Tsutsumi, S.; Sone, J.; Ishikawa, T.; Imanishi, T.; Koizumi, M. *Bioorg. Med. Chem. Lett.* **2002**, *12*, 73–76.

(22) Koizumi, M.; Morita, K.; Daigo, M.; Tsutsumi, S.; Abe, K.; Obika, S. i.; Imanishi, T. *Nucl. Acids Res.* **2003**, *31*, 3267–3273.

TABLE 1. Experimental $^3J_{\text{H,H}}$ Vicinal Proton Coupling Constants,^{10,12,14,17,21} Corresponding *ab Initio* and MD (Highlighted in Blue) $\phi_{\text{H,H}}$ Torsions, and Respective Theoretical $^3J_{\text{H,H}}$ Obtained Using the Haasnoot–de Leeuw–Altona Generalized Karplus Equation^{44,45} Taking into Account the β Substituent Correction^{a,b}

Compounds (see Fig. 1)	Vicinal proton coupling	Torsion ($\phi_{\text{H,H}}$)	$^3J_{\text{H,H}}$, calc. Hz	$^3J_{\text{H,H}}$, exp. Hz	$\phi_{\text{H,H}}$ ($^\circ$), <i>ab initio</i>	$\phi_{\text{H,H}}$ ($^\circ$), MD	$\phi_{\text{H,H}}$ ($^\circ$), exp.	$\Delta^3J_{\text{H,H}}$, Hz
(A) Azetidine-T	$^3J_{\text{H-2',H-3'}}$	H2'-C2'-C3'-H3'	5.75	5.60	35.22	23.6 ± 13.6	36.5 to 36.6	0.15
	$^3J_{\text{H-3',H-4'}}$	H3'-C3'-C4'-H4'	7.59	8.31	-152.98	-152.0 ± 19.5	-149.9 to -150.0	-0.72
(B) Oxetane-T	$^3J_{\text{H-2',H-3'}}$	H2'-C2'-C3'-H3'	4.27	3.86	43.27	36.2 ± 9.5	46.1 to 46.3	0.41
	$^3J_{\text{H-3',H-4'}}$	H3'-C3'-C4'-H4'	8.62	8.00	-163.13	-160.4 ± 12.4	-148.3 to -148.4	0.62
(C) Aza-ENA-T	$^3J_{\text{H-2',H-3'}}$	H2'-C2'-C3'-H3'	3.77	3.9	49.69	43.5 ± 5.6	48.7 to 48.9	-0.13
	$^3J_{\text{H-7',H-6'}}$	H7'-C7'-C6'-H6'	7.16	6.7	41.37	42.3 ± 8.2	43.8 to 44.0	0.46
	$^3J_{\text{H-7'',H-6'}}$	H7''-C7''-C6'-H6'	11.37	13.0	158.12	152.5 ± 8.0	172.5 to 176.4	-1.63
	$^3J_{\text{H-7'',H-6''}}$	H7''-C7''-C6'-H6''	5.04	4.7	40.01	36.1 ± 8.0	42.6 to 42.8	0.34
(D) ENA-T	$^3J_{\text{H-2',H-3'}}$	H2'-C2'-C3'-H3'	3.19	3.20	51.16	49.3 ± 5.9	51.0 to 51.1	-0.01
	$^3J_{\text{H-7',H-6'}}$	H7'-C7'-C6'-H6'	7.91	7.50	37.92	39.0 ± 8.9	40.2 to 40.4	0.41
	$^3J_{\text{H-7'',H-6'}}$	H7''-C7''-C6'-H6'	11.30	11.70	156.84	155.4 ± 8.7	160.8 to 161.0	-0.40
	$^3J_{\text{H-7'',H-6''}}$	H7''-C7''-C6'-H6''	5.12	3.80	38.39	38.3 ± 8.3	48.2 to 48.4	1.32

^a Optimized parameters $N_{\text{aza}}/N_{\text{amino}}$ (1.305) and O_{oxe} (1.480) are employed for constrained heterocycles containing O_{oxe} or N_{aze} -type atoms resulting in group electronegativities of C2' being 0.408 and 0.369 for the H-3'-H-4' vicinal proton couplings in azetidine-T and oxetane-T, respectively. ^b Average rmsd between experimental and calculated couplings was 0.56 Hz.

nature of a modified residue on the thermal stability the BNA/LNA and ENA duplexes and triplexes²² varies, and it depends not only on the type of sugar constraints but also on the nature of the nucleobase.^{9–12} Thus, in general, the stability of the AON/RNA duplexes change in the following order: thyminy^{9–12} < cytosiny^{10,12} < adeniny^{10,12} \approx guaniny^{10,12}. Other important factors in the observed variation of the thermal stability of AON/RNA (DNA) duplexes are the position of the modification site in the AON strand and the sequence content around the modified nucleotide.^{5,7,18,21–23} McTigue et al.²⁴ have shown the substantial dependence of the LNA-modified DNA/DNA duplex stability on the neighboring sequence for all of the LNA bases which resulted²⁴ in the somewhat unexpected conclusion that LNA purines contribute significantly less enhanced stability than do pyrimidines. LNA-A in particular had been shown to have the smallest effect of the four; and in terms of ΔT_m the average stability increments were ordered LNA-A ($\Delta T_m = 2.11 \pm 1.30$ °C)²⁴ < LNA-G ($\Delta T_m = 2.83 \pm 1.75$ °C)²⁴ < LNA-T ($\Delta T_m = 3.21 \pm 1.41$ °C)²⁴ < LNA-C ($\Delta T_m = 4.44 \pm 1.46$ °C).²⁴

Physicochemical properties of the constrained 1',2'- and 2',4'-fused nucleosides (Figure 1), studied here as a monomer units, are expected to have profound effect on the properties of ON where the modified nucleotides could be incorporated.^{25–31}

(23) Hamada, M.; Ohtsuka, T.; Kawaida, R.; Koizumi, M.; Morita, K.; Furukawa, H.; Imanishi, T.; Miyagishi, M.; Taira, K. *Antisense Nucleic Acid Drug Dev.* **2002**, *12*, 301.

(24) McTigue, P. M.; Peterson, R. J.; Kahn, J. D. *Biochemistry* **2004**, *43* (18), 5388–5405.

(25) Helene, C. *Eur. J. Cancer* **1991**, *27*, 1466.

(26) Vasquez, K. M.; Wilson, J. *Trends Biochem. Sci.* **1998**, *23*, 4.

(27) Chech, T. R.; Zaug, A. J.; Grabowski, P. J. *Cell* **1981**, *27*, 487.

(28) Kruger, K.; Grabowski, P. J.; Zaug, A. J.; Sands, J.; Gottschling, D. E.; Chech, T. R. *Cell* **1982**, *31*, 147.

(29) Schubert, S.; Gül, D. C.; Grunert, H. P.; Grunert, H.; Erdmann, V. A.; Kurreck, J. *Nucl. Acids Res.* **2003**, *31*, 5982.

Rigidity of the conformationally constrained nucleotides influences structural and conformational preorganization of modified ON single strand.^{32–35} This may influence not only stability of their duplexes with complementary DNA or RNA strand^{1,11,20,35,36} but also recognition by and interaction with the target enzyme, such as RNase H in the antisense action^{1,20,30,37,38} or the recruitment of endonucleases in the RISC complex in RNAi³⁹ or, alternatively, control the stability toward endo-/exo-nucleases.^{7,8,16,18,21–23,33,37,40} Thus, a conformationally constrained nucleotide may be able to tune the dynamics of the double-stranded homo and heteroduplexes to steer the substrate specificity in the antisense^{1,30,38} or RNAi action.^{31,41–43}

Results and Discussion

Parametrization of the Haasnoot–de Leeuw–Altona generalized Karplus equation^{44,45} has been performed to refine and

(30) Crooke, S. T. *Annu. Rev. Med.* **2004**, *55*, 61–95.

(31) Fire, A.; Xu, S.; Motgomery, M. K.; Kostas, S. A.; Driver, S. E.; Mello, C. C. *Nature* **1998**, *391*, 806.

(32) Isaksson, J.; Acharya, S.; Barman, J.; Cheruku, P.; Chattopadhyaya, J. *Biochemistry* **2004**, *43* (51), 15996.

(33) Surono, A.; Van Khanh, T.; Takeshima, Y.; Wada, H.; Yagi, M.; Takagi, M.; Koizumi, M.; Matsuo, M. *Hum. Gene Ther.* **2004**, *15*, 749.

(34) Berger, I.; Tereshko, V.; Ikeda, H.; Marquez, V. E.; Egli, M. *Nucl. Acids Res.* **1998**, *26* (10), 2473–2480.

(35) Egli, M.; Minasov, G.; Teplova, M.; Kumar, R.; Wengel, J. *Chem. Commun.* **2001**, 651–652.

(36) Isaksson, J.; Plashkevych, O.; Pradeepkumar, P. I.; Chatterjee, S.; Barman, J.; Pathmasiri, W.; Shrivastava, P.; Petit, C.; Chattopadhyaya, J. *J. Biomol. Struct. Dyn.* **2005**, *23* (3), 299.

(37) Yazbeck, D. R.; Min, K.-L.; Damha, M. J. *Nucl. Acids Res.* **2002**, *30* (14), 3015–3025.

(38) Brenda, F. B.; Brett, P. M. *Biochem. Biophys. Acta* **1999**, *1489* (1), 3–18.

(39) Hannon, G. J. *Nature* **2002**, *418*, 244–251.

(40) Yagi, M.; Takeshima, Y.; Surono, A.; Takagi, M.; Koizumi, M.; Matsuo, M. *Oligonucleotides* **2004**, *14*, 33.

extract structural information from the NMR data of 2',4'-fused LNA-T, ENA-T, 2'-amino-LNA-T, and aza-ENA-T nucleosides (compounds **A–F** in Figure 1), employing ab initio and molecular dynamics (MD) methods as well as experimental vicinal proton coupling constants ($^3J_{\text{H,H}}$) (collected in Tables 1 and 2, Figure 2, and Figure S11 in the Supporting Information) from NMR experiments.^{10,12,14,17,21}

A. Generalized Karplus Parametrization. The assignments from reported^{10,12,14,17,21} 1D and 2D NMR spectra as well as the experimental coupling constants of compounds **A–D** in Figure 1 have been used to optimize the group electronegativity parameter of the Haasnoot–de Leeuw–Altona generalized Karplus equation^{44,45} for the endocyclic nitrogen atom (N_{aze}) connected to C2' in azetidine-, aza-ENA-, and 2'-amino-LNA-types of modifications as well as for the endocyclic oxygen (O_{oxe}) in the 1',2'-bridged-oxetane-type and the 2'-O,4'-C-methylene(ethylene) ring the ENA- and LNA-type nucleosides. The full set of these compounds (Table 1) has been employed in the least-square fitting numerical grid procedure to obtain optimized Karplus parameters using a set of experimental $^3J_{\text{H,H}}$ coupling constants and corresponding torsions from the ab initio calculations. Experimental NMR data have been further rationalized using structural information from (i) 6-31G** Hartree–Fock optimized ab initio gas-phase geometries by GAUSSIAN 98;⁴⁶ (ii) NMR constrained molecular dynamics simulation which consisted of 0.5 ns (10 steps) simulated annealing (SA) followed by 0.5 ns NMR constrained simulations at 298 K to yield NMR defined molecular structures of the compounds **A–F** in Figure 1; and (iii) 2 ns constraints-free MD simulations of all compounds in question. The MD simulations were performed using AMBER 7⁴⁷ force field, and explicit TIP3P⁴⁸ aqueous medium (see details in Experimental Section). Relevant vicinal proton $^3J_{\text{H}_1, \text{H}_2}$, $^3J_{\text{H}_2, \text{H}_3}$, and $^3J_{\text{H}_3, \text{H}_4}$ coupling constants have been back-calculated from the corresponding theoretical torsions employing Haasnoot–de Leeuw–Altona generalized Karplus equation^{44,45} taking into account β substituent correction

$$^3J = P_1 \cos^2(\phi) + P_2 \cos(\phi) + P_3 + \sum (\Delta\chi_i^{\text{group}}(P_4 + P_5 \cos^2(\xi_i\phi + P_6|\Delta\chi_i^{\text{group}}|)))$$

where $\Delta\chi_i^{\text{group}} = \Delta\chi_i^{\alpha\text{-substituent}} - P_7 \sum \Delta\chi_i^{\beta\text{-substituent}}$ and the $\Delta\chi_i$ are taken as Huggins electronegativities.⁴⁹ Specifics of the endocyclic heteroatoms in our set of compounds required reparametrization of the group electronegativities for $N_{\text{aza}}/(N_{\text{amino}})$ and O_{oxe} atoms which has been achieved by solving the generalized Karplus equation^{44,45} parametrized by $P_1 = 13.70$, $P_2 = -0.73$, $P_3 = 0.00$, $P_4 = 0.56$, $P_5 = -2.47$, $P_6 = 16.90$, $P_7 = 0.14$ (parameters from ref 45) for the set of the observed vicinal coupling constants of the oxetane and azetidine con-

strained compounds as well as ENA-T and aza-ENA-T yielded 1.305 and 1.480 as the group electronegativities for $N_{\text{aza}}/(N_{\text{amino}})$ and O_{oxe} , respectively. The use of β -substitution correction lead to electronegativities of C2' groups of azetidine- and oxetane-T to become 0.408 and 0.369, respectively. Other group electronegativities were kept unmodified, and their respective standard values⁴⁵ were as follows: C1' (0.738), O4' (1.244), C3' (0.162), C2' (0.099), O3' (1.3 for OH), C4' (0.106), C5' (0.218). Average root-mean-square difference (RMSd) between calculated and observed experimental vicinal coupling constants was 0.56 Hz for the set of compounds used for the parametrization.

B. Molecular Structure of the Conformationally Constrained 1',2'- and 2',4'-Fused Nucleosides. IUPAC recommended definitions of torsional angles are used throughout the text (see Figure S10 in SI).

1. Sugar Pucker. Direct effect of the chemical modification of sugar moiety by bridging C1' and C2' or C2' and C4' atoms is the restriction of the internal dynamics of this moiety (see Tables 1 and 2, Figure 2, and Figure S11 in the Supporting Information) which locks the sugar moieties into the *North-East* type conformation in the 1',2'-fused azetidine and oxetane-T and to the relatively pure *North* type C3'-*endo* in the 2',4'-bridged LNA, ENA, and their 2'-amino analogues (Table 2, Figure 2). Compared to the ENA, LNA, and their 2'-amino analogues, the 1',2'-fused azetidine and oxetane modifications impose weaker constraints on the sugar pucker resulting in higher dynamics of the sugar moiety and broader conformational hyperspace accessible. Thus, the spreads of the pseudorotational phase angles (P)⁵⁰ of the 1',2'-fused systems are higher, and the puckering amplitudes (ϕ_m)⁵⁰ are lower compared to those of the 2',4'-fused ENA- and LNA-type counterparts, $P = 42\text{--}44^\circ$, $\phi_m = 29\text{--}34^\circ$ vs $P = 12\text{--}19^\circ$, $\phi_m = 46^\circ$ (ENA-T), 56° (LNA-T) (Table 2, Figure S11 in SI). Higher variations of P ($20\text{--}27^\circ$ vs $5\text{--}8^\circ$ in LNA-T and ENA-T) as well as higher amplitude of motion of ϕ_m ($9\text{--}18^\circ$ vs $\sim 3^\circ$ in LNA-T and ENA-T) along the MD trajectories indicated broader and uniquely defined (although overlapping with that of the ENA-T and LNA-T) conformational hyperspace available. Higher rigidity and, correspondingly, relatively lower dynamics of the sugar moiety in 2',4'-fused systems are indirectly confirmed by virtually identical average P and ϕ_m obtained for the LNA-T and ENA-T from ab initio and MD simulations, while the difference of $\sim 10^\circ$ in P and ϕ_m has been observed for the 1',2'-fused systems.

2. Backbone Torsion Angles γ and δ . During the first 0.6 ns of the MD simulations the backbone γ torsions appeared to be in *gauche* conformation in both the 1',2'- and 2',4'-fused systems (61° for azetidine and oxetane, 63° for ENA-T and 2'-amino ENA-T, 66° for LNA-T and 2'-amino LNA-T, Table 2). However, longer MD simulations revealed that γ torsion in the LNA- and ENA-type modified nucleosides tends to undergo sudden and apparently reversible (LNA-T) or irreversible (aza-ENA-T, 2'-amino-LNA-T) transition tuning γ into *trans*⁺/*trans*⁻ (*t*⁺/*t*⁻) conformation. Energetically this transition appeared favorable as the average total energy of the system decreased by 1–3 kcal/mol in LNA-T, 2'-amino-LNA-T, and aza-ENA-T compounds (Figure S11 in SI). However, this decrease is much lower than the amplitude of energy fluctuation ($\sim 7\text{--}15$ kcal/mol) during the MD runs which probably explains the abruptness of such transition. No γ *gauche/trans* transition has however been observed in the simulations of 1',2'-oxetane- and 1',2'-

(41) Hutvagner, G.; Zamore, P. D. *Science* **2002**, *297*, 2056.

(42) Novina, C. D.; Sharp, P. A. *Nature* **2004**, *430*, 161–164.

(43) Xia, J.; Noronha, A.; Toudjarska, I.; Li, F.; Akinc, A.; Braich, R.; Frank-Kamenetsky, M.; Rajeev, G. K.; Egli, M.; Manoharan, M. *Chem. Biol.* **2006**, *1* (3), 176–183.

(44) Altona, C.; Sundaralingam, M. *J. Am. Chem. Soc.* **1972**, *94* (23), 8205–1822.

(45) Haasnoot, C. A. G.; de Leeuw, F. A. A. M.; Altona, C. *Tetrahedron* **1980**, *36*, 2783–2792.

(46) Frisch, M. J. et al., *Gaussian 98 (Revision A.6)*; Gaussian, Inc: Pittsburgh, PA, 1998.

(47) Case, D. A.; et al. *AMBER 7*; University of California: San Francisco, 2002.

(48) Jorgensen, W. L.; Chandrasekhar, J.; Madura, J. D.; Impey, R. W.; Klein, M. L. *J. Chem. Phys.* **1983**, *79*, 926–935.

(49) Huggins, M. L. *J. Am. Chem. Soc.* **1953**, *75*, 4123.

(50) Cremer, D.; Pople, J. A. *J. Am. Chem. Soc.* **1975**, *97*, 1354–1358.

TABLE 2. Sugar Torsions (ν_0 - ν_4), Pseudorotational Phase Angle (P),⁵⁰ Sugar Puckering Amplitude (ϕ_m),⁵⁰ Backbone (γ , δ), and Glycoside Bond (χ) of the Oxetane- and Azetidino-T, LNA-T, ENA-T and Their Nitrogen Containing Analogues (Compounds A–F in Figure 1), as Well as Selected Torsions (C3'–C2'–O2'–C7' and C3'–C4'–C6'–C7') Characterizing the Modifying Heterocycle in the Aza-ENA-T, ENA-T, 2'-Amino-LNA-T, and LNA-T (Compounds C–F in Figure 1)^a

Torsions	(A)		(B)		(C)		(D)		(E)		(F)	
	Value	Standard Deviation	Value	Standard Deviation	Value	Standard Deviation	Value	Standard Deviation	Value	Standard Deviation	Value	Standard Deviation
ν_0 : C4'-O4'-C1'-C2'	-13.22	(-6.4 ± 12.2)	-14.30	(-10.5 ± 9.1)	-0.91	(-0.5 ± 6.8)	-1.05	(5.8 ± 6.0)	-1.60	(-0.7 ± 5.5)	-1.62	(0.1 ± 5.6)
ν_1 : O4'-C1'-C2'-C3'	-6.16	(-8.9 ± 6.3)	-8.89	(-10.2 ± 6.2)	-28.21	(-29.5 ± 5.5)	-28.10	(-34.3 ± 4.9)	-34.36	(-37.7 ± 4.6)	-34.89	(-37.8 ± 4.7)
ν_2 : C1'-C2'-C3'-C4'	20.94	(19.3 ± 11.9)	26.03	(24.9 ± 7.5)	43.87	(44.8 ± 3.4)	43.70	(46.1 ± 3.4)	52.56	(56.0 ± 2.8)	53.15	(55.3 ± 3.0)
ν_3 : C2'-C3'-C4'-O4'	-28.96	(-24.6 ± 18.1)	-34.88	(-32.4 ± 10.7)	-45.14	(-47.6 ± 4.0)	-44.84	(-45.3 ± 4.0)	-54.55	(-59.1 ± 3.3)	-54.91	(-57.8 ± 3.4)
ν_4 : C3'-C4'-O4'-C1'	27.18	(19.8 ± 19.4)	31.52	(27.5 ± 11.6)	29.65	(30.5 ± 6.1)	28.88	(25.2 ± 5.5)	36.99	(39.5 ± 5.2)	37.37	(38.1 ± 5.3)
Phase angle P	44.44	(37.2 ± 27.0)	41.87	(36.6 ± 20.7)	19.38	(19.4 ± 8.0)	19.14	(12.1 ± 7.2)	19.97	(19.6 ± 5.3)	19.84	(18.8 ± 5.4)
Puckering ampli. ϕ_m	29.33	(25.1 ± 18.2)	34.96	(32.9 ± 9.5)	46.50	(48.0 ± 3.4)	46.26	(47.6 ± 3.3)	55.92	(59.7 ± 2.8)	56.50	(58.7 ± 2.9)
γ : O5'-C5'-C4'-C3'	61.33	(54.8 ± 10.8)	60.73	(57.9 ± 10.7)	64.53	(53.1 ± 10.7)	63.89	(57.3 ± 9.3)	66.23	(57.2 ± 19.6)	66.62	(58.1 ± 10.3)
δ : C5'-C4'-C3'-O3'	89.94	(90.1 ± 14.9)	88.57	(90.1 ± 14.9)	75.61	(74.5 ± 5.9)	76.02	(73.5 ± 5.8)	66.61	(63.9 ± 5.7)	65.83	(63.0 ± 5.8)
χ : O4'-C1'-N1-C2	-89.06	(-79.7 ± 11.1)	-88.96	(-79.6 ± 12.1)	-156.21	(-157.2 ± 10.8)	-150.99	(-161.5 ± 10.9)	-161.37	(-167.7 ± 8.7)	-162.40	(-167.6 ± 9.9)
C3'-C2'-O2' (N2)-C7' (C6')					68.08	(67.0 ± 4.8)	65.87	(65.1 ± 5.6)	43.10	(39.9 ± 4.4)	38.92	(40.0 ± 5.1)
C3'-C4'-C6'-C7' (O2'/N2)					-57.49	(-55.5 ± 5.2)	-56.36	(-56.1 ± 5.4)	-31.48	(-36.0 ± 4.7)	-34.71	(-35.6 ± 4.6)

^a The structural parameters are obtained from the ab initio molecular structures as well as from the last 0.5 ns of unconstrained MD simulations (average values and standard deviations are shown in parentheses and highlighted in blue) of the respective nucleosides.

Azetidine-T (A)	Oxetane-T (B)	Aza-ENA-T (C)	ENA-T (D)	2'-amino LNA-T (E)	LNA-T (F)
RMSd = 0.569 (0.194, 0.739)	RMSd = 0.527 (0.171, 0.687)	RMSd = 0.433 (0.092, 0.656)	RMSd = 0.462 (0.078, 0.646)	RMSd = 0.567 (0.100, 0.699)	RMSd = 0.628 (0.089, 0.629)

FIGURE 2. Superposition of 10 randomly selected structures during the last 400 ps of the unconstrained 2 ns MD simulations of azetidine-T, oxetane-T, aza-ENA-T, ENA-T, 2'-amino-LNA-T, and LNA-T (compounds (A–F) in Figure 1). Total average rmsd (in Å) are shown for all heavy atoms (marked in black) as well as for the heavy atoms in sugar and piperidino moieties (in parentheses marked in red), and the base atoms (in parentheses marked in blue).

azetidine-T nucleosides, while a sudden $\sim 60^\circ$ flip occurred during 2 ns simulations (Figure S11 in SI) of ENA-T (γ in t^+/t^- conformation for ~ 10 ps), aza-ENA-T (about 20% of the time in MD simulation), LNA-T (about 10% of the simulation's time), and 2'-amino-LNA-T (almost 50% of the simulation's time). Attempts to revert γ *gauche*⁻ into γ *trans* conformation using the simulated annealing (SA) protocol with imposed NMR constraints (simulation time of 10 SA steps plus following MD simulation at 293 K was 1 ns) proved unsuccessful. Thus, in case of amino analogues of ENA-T and LNA-T the most stable conformation of γ torsion appeared to be t^+/t^- contrary to canonical *gauche*⁺ conformation observed for unmodified nucleotides in polynucleotides.⁵²

Another important backbone torsion δ has also been affected by the sugar modifications which lead to a significant difference (Table 2) of about 10° between δ torsions of LNA-T and ENA-T nucleosides ($\delta = 66^\circ$ and 76° , respectively, which is consistent with 66° and 77° reported by Wengel et al.¹² for LNA and Morita et al.¹⁶ for ENA). Least puckered in this series of compounds 1',2'-fused azetidine and oxetane modified nucleosides have been found rotated around the C4'–C3' bond even further by 13° ($\delta = 89^\circ$). The amplitudes of fluctuation of the δ torsion in the 1',2'-constrained azetidine-T and oxetane-T nucleosides during MD trajectories have been found to be as much as $\sim 15^\circ$, which is almost tripled compared to those of the 2',4'-fused systems ($\sim 6^\circ$, Table 2). These fluctuations of the δ torsion in the 1',2'-fused nucleosides are also characterized by sudden and frequent variations of up to $\sim 120^\circ$ (Figure S11 in SI) along the respective MD trajectories, compared to the maximum variations below 20° in the 2',4'-fused systems (Table 2, Figure S11 in SI).

(51) Chatterjee, S.; Pathmasiri, W.; Plashkevych, O.; Honcharenko, D.; Varghese, O. P.; Maiti, M.; Chattopadhyaya, J. *Org. Biomol. Chem.* **2006**, *4*, 1675–1686.

(52) Várnai, P.; Djuranovic, D.; Lavery, R.; Hartmann, B. *Nucleic Acids Res.* **2002**, *30* (24), 5398–5406.

3. Glycoside χ Torsions. Relative orientation of the nucleobase to the sugar moiety has been found to be greatly influenced by the type of modification, with the 1',2'-constrained and 2',4'-constrained nucleosides, forming two distinct groups. The 1',2'-fused four-membered azetidine and oxetane rings lead not only to a quite unusual near- 270° (*syn*⁻/*anti*⁺) orientation of the glycoside characterized by bond torsion χ (O4'–C1'–N1–C2) which in LNA-T, ENA-T, and their 2'-amino analogues has been found in the range of $-160^\circ \pm 11^\circ$ (ENAs) and $-167^\circ \pm 9^\circ$ (LNAs). This *anti*⁻ orientation of the glycoside is contrary to that observed in azetidine and oxetane modified nucleosides. The magnitude of variation of the χ values is relatively high (9 – 12°)

in all considered modified nucleosides but nevertheless the nucleobase conformation changes in a relatively narrow region of corresponding *anti*⁻ (ENA-, LNA-type) or *syn*⁻ (1',2'-bridged) orientation domain. The *syn*⁻ orientation of nucleobase in 1',2' azetidine and oxetane thymidines indicates that sugar modification may cause a distortion of the typical Watson–Crick base pairing in the DNA and/or RNA duplexes, which is probably leading to the observed thermal destabilization of the duplexes.^{9–11,20}

4. pK_a Variation of the 1-Thyminyll Moiety as a Result of Alteration of the Electronic Character of the Conformationally Constrained Endocyclic-Amino Group in the Sugar Moiety. Results of the NMR titration experiments show that the molecular nature of the sugar constraint has a profound influence both on the pK_a of the endocyclic-amino group in the sugar moiety (2'-N analogues) as well as on the pK_a of the N³ of the constituent 1-thyminyll moiety, depending both upon the linkage sites (1',2'- vs 2',4'-fused) and the ring-size (4-, 5-, or 6-membered) of the sugar constraint (Table 3). The pH-dependent ¹H chemical shift measurements showed (Tables 3 and 4, Figure S1–S9 in SI) that the endocyclic azetidine-amino group in four-membered azetidine-T [compound A in Figure

TABLE 3. Theoretical Proton Affinities (PA), Thermodynamics Circle's Components Enthalpies (ΔH°), Gibbs Free Energies (Gas Phase and Solvation, ΔG° and ΔG_s° , Respectively), and the Theoretical pK_a Values of the Oxetane- and Azetidene-T, LNA-T, ENA-T, and Their Nitrogen Containing Analogues (Compounds A–F in Figure 1) as Well as the Available Experimental pK_a Values

Modified nucleoside and protonation/deprotonation site	ΔH , BH (gas), a.u.	ΔG , BH (gas), a.u.	ΔG_s , BH (aq), kcal/mol.	ΔH , B (gas), a.u.	ΔG , B (gas), a.u.	ΔG_s , B (aq), kcal/mol.	PA (gas) kcal/mol	$\Delta\Delta G_{\text{gas}}^\circ$, kcal/mol	$\Delta\Delta G_s^\circ$, kcal/mol	pK_a (calc, raw)	pK_a^d (calc, proj.)	pK_a^4 (exp)
Hartree-Fock, 6-31 G**												
Azetidine-T N ³	-962.690147	-962.754509	-16.82	-962.124209	-962.187689	-69.14	355.13	303.37	-52.32	25.19	9.2 (9.7)	9.14
N _{aza}	-963.052553	-963.118856	-76.23	-962.690147	-962.754509	-16.82	227.41	288.04	59.41	13.96	6.2 (4.4)	6.07
Oxetane-T N ³	-982.528975	-982.593174	-15.38	-981.967389	-982.030678	-65.63	352.40	302.72	-50.25	24.72	9.1 (9.5)	
Aza-ENA-T N ³	-1001.729046	-1001.794089	-15.22	-1001.159097	-1001.223755	-67.20	357.65	305.91	-51.98	27.05	9.7 (10.6)	9.60
N _{aza}	-1002.099533	-1002.165728	-70.81	-1001.729046	-1001.794089	-15.22	232.48	288.80	55.59	14.52	6.4 (4.7)	6.69
ENA-T N ³	-1021.561546	-1021.626664	-15.62	-1020.991761	-1021.057103	-68.64	357.55	304.39	-53.02	25.93	9.4 (10.1)	
2'-amino-LNA-T N ³	-962.708379	-962.771436	-16.92	-962.139546	-962.202259	-69.23	356.95	304.85	-52.31	26.28	9.5 (10.2)	9.50
N _{amino}	-963.073777	-963.137990	-75.19	-962.708379	-962.771436	-16.92	229.29	288.29	58.27	14.14	6.3 (4.5)	6.17
LNA-T N ³	-982.542989	-982.606144	-16.78	-981.975322	-982.038099	-69.30	356.22	303.93	-52.52	25.60	9.3 (9.9)	
B3LYP, 6-31++G**												
Azetidine-T N ³	-968.362289	-968.429386	-18.66	-967.822520	-967.888694	-68.11	338.71	289.84	49.45	15.27	9.1	9.14
N _{aza}	-968.714095	-968.782183	-80.27	-968.362289	-968.429386	-18.66	220.76	282.99	61.61	10.26	6.6	6.07
Oxetane-T N ³	-988.237686	-988.304518	-16.87	-987.701383	-987.767500	-64.45	336.54	289.40	-47.58	14.95	9.0	
Aza-ENA-T N ³	-1007.680499	-1007.748302	-16.58	-1007.136450	-1007.204590	-66.39	341.40	291.37	-49.81	16.40	9.6	9.60
N _{aza}	-1008.038226	-1008.107053	-73.37	-1007.680499	-1007.748302	-16.58	224.48	281.91	56.79	9.46	6.2	6.69
ENA-T N ³	-1027.549737	-1027.617466	-16.24	-1027.007823	-1027.075674	-66.11	340.06	290.11	-49.87	15.47	9.2	
2'-amino-LNA-T N ³	-968.377594	-968.443547	-18.55	-967.834534	-967.900426	-68.39	340.78	290.97	-49.84	16.11	9.5	9.50
N _{amino}	-968.730674	-968.797996	-78.16	-968.377594	-968.443547	-18.55	221.56	282.03	59.61	9.55	6.2	6.17
LNA-T N ³	-988.248951	-988.315078	-17.92	-987.706703	-987.772888	-68.10	340.27	290.05	-50.18	15.43	9.2	

^a Projected pK_a values are obtained using the empirical correlation $pK_a(\text{exp}) = A \times pK_a(\text{calc}) + B$, where, in the case of Hartree-Fock 6-31G** calculations, the correlation coefficients were $A = 0.2623$ (std err. 0.0120) and $B = 2.5683$ (std err. 0.2534) and, in the case of B3LYP, 6-31++G** calculations, $A = 0.4995$ (std err. 0.0475) and $B = 1.4505$ (std err. 0.6274). Values in parentheses are obtained using coefficients $A = 0.4690$ and $B = -2.1087$ as reported in ref 51. ^b Experimental pK_a values are obtained from the Hill plot analysis (see Experimental Section for details).

TABLE 4. pK_a and $\Delta G^\circ_{pK_a}$ of the 2'-Amino Protonation and Thymidine N^3 Deprotonation Calculated from Results of the Hill Plot Analysis of 2'-Amino-T, 1',2'-Azetidine-T (Compound A in Figure 1), Aza-ENA-T (C), and 2'-Amino-LNA-T (E)^a

Compounds	pK_a (2'-amino)	$\Delta G^\circ_{pK_a}$ (2'-amino) kJmol ⁻¹	pK_a (N^3)	$\Delta G^\circ_{pK_a}$ (N^3) kJ mol ⁻¹	$\Delta\Delta G^\circ_{pK_a}$ (base-pairing energy) [kJ mol ⁻¹] ^b
	5.99 (0.02)	34.2	9.52 (0.02)	54.3	33.0
	6.07 (0.03)	34.6	9.14 (0.02)	52.4	31.1
	6.17 (0.02)	35.2	9.50 (0.01)	54.2	32.9
	6.69 (0.02)	38.2	9.60 (0.02)	54.8	33.5

^a Base-pair free energy $\Delta\Delta G^\circ_{pK_a}$ is estimated as a difference in $\Delta G^\circ_{pK_a}$ of the hydrogen bond donor and $\Delta G^\circ_{pK_a}$ of acceptor (ribo-adenosine). The $\Delta\Delta G^\circ_{pK_a}$ represents the average of the base-pairing energy values calculated from the pK_a values obtained from the Hill plot analysis. These $\Delta\Delta G^\circ_{pK_a}$ values are to be compared to $\Delta\Delta G^\circ_{pK_a}$ of the native deoxy-T:ribo-A base pair equal to 36.4 kJ mol⁻¹. ^b $\Delta\Delta G^\circ_{pK_a}$ (base-pairing energy) = $\Delta G^\circ_{pK_a}$ (donor-T) - $\Delta G^\circ_{pK_a}$ (acceptor-A). A more positive value of $\Delta\Delta G^\circ_{pK_a}$ indicates less strong base-pairing. To estimate the $\Delta\Delta G^\circ_{pK_a}$, the acceptor's pK_a of 3.73 ($\Delta G^\circ_{pK_a}$ = 21.3 kJ mol⁻¹) was used as obtained for the 3',5'-bis-ethylphosphate ribo-adenosine.⁵⁵

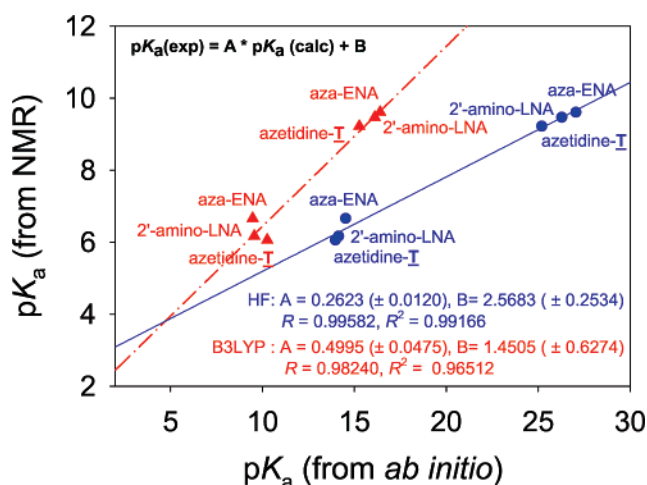


FIGURE 3. Correlation between calculated and experimental pK_a of endocyclic amino groups in azetidine-T (compound (A) in Figure 1), aza-ENA (C), and 2'-amino-LNA (E). B3LYP/6-31++G** (red triangles, dash-dotted red line) and HF/6-31G** (blue circles, solid blue line) levels of ab initio calculations have been employed.

1] has pK_a of 6.06, which is 0.5 pK_a units more acidic compared to that of piperidino-amino group in aza-ENA-T (pK_a 6.66) (C), whereas the pyrrolidino-amino group in 2'-amino-LNA-T (E) has a pK_a of 6.17. Thus, as the ring-size decreases from

6-membered (aza-ENA-T) to 5-membered (2'-amino-LNA-T) to four-membered (azetidine-T) the basicity of the of the endocyclic-amino group decreases, which in turn causes a decrease in the basicity of the N^3 (T) (Figure 3, Table 3, Figures S9a,b in SI): pK_a of N^3 in aza-ENA-T > pK_a of N^3 in 2'-amino-LNA-T > pK_a of N^3 in azetidine-T. Clearly, the more basic character of the piperidino-amino group in aza-ENA-T compared to pyrrolidino-amino group in 2'-amino-LNA-T is a result of weaker inductive effect of O4' in the former compared to that in the latter.⁵³

Interestingly, although the endocyclic 2'-amino group in 1',2'-azetidine-T is a secondary amine, it shows the pK_a of primary amine of 2'-amino-T (Table 4, Figure 9a,b in SI). The measured pK_a of endocyclic 2'-amino group in 2'-amino-LNA-T is also close to that value being only 0.1 pK_a unit more basic than that of the endocyclic amino in 1',2'-azetidine-T while pK_a of endocyclic 2'-amino group in aza-ENA-T is found to be 0.51 pK_a unit more basic than that of the 2'-amino in 2'-amino-LNA-T. Overall the endocyclic O4' and the 1-thyminy moiety have a net electron withdrawing effect on the pK_a of the fused azetidine, which can be concluded comparing the pK_a of the endocyclic amine protonation of azetidine-T (pK_a = 6.07, Table 4, Figures 9a,b in SI) to that of alkyl-azetidine (azelnidipine)⁵⁴

(53) Sandström, A.; Kwiatkowski, M.; Chattopadhyaya, J. *Acta Chem. Scand.* **1985**, B39, 273–290.

($pK_a = 7.89$) which is $1.82 pK_a$ ($\Delta\Delta G^\circ_{pK_a} = 10.9 \text{ kJ mol}^{-1}$ or $2.6 \text{ kcal mol}^{-1}$) unit more basic.

The nucleobase pK_a s in the 2'-*N*-modified nucleosides are found to be correlated with the pK_a s of the endocyclic 2'-amino group (Table 4). Interestingly, the size of the fused ring of the *N*-heterocycle (and correspondingly the flexibility of the fused system) is correlated with the pK_a of the endocyclic amine or the N^3 of 1-thymine base (Table 4), showing that the pK_a of the endocyclic amine decreases as the ring size of the *N*-heterocycle becomes smaller. The same trend is predicted (Table 3) for the endocyclic 2'-oxygen containing nucleosides where the HF/6-31G** calculated nucleobase pK_a s are as follows: oxetane-T (9.05) **B** < azetidine-T (pK_a 9.17) **A** < LNA (pK_a 9.28) **F** < ENA (pK_a 9.37) **D** < 2'-amino-LNA (pK_a 9.46) **E** < aza-ENA (pK_a 9.66) **C**, which is consistent with the experimental pK_a s available so far (Table 3). The calculated pK_a of N^3 of the 1-thymine moiety in the endocyclic 2'-oxygen containing nucleosides **A–F** in Figure 1 show consistently relatively lower pK_a values (up to $0.5 pK_a$ units) compared to that of the nitrogen-containing analogues. This is in line with the expected less constraining ability of nitrogen atom, having relatively lower electronegativity, resulting in higher amplitude of internal motions (Tables 3 and 4, Figures S9ab in SI) compared to that in the 2'-endocyclic oxygen analogues.

The HF/6-31G** calculated and experimental pK_a values have however been found to be linearly correlated ($R = 0.991$, $pK_a(\text{expt}) = A \times pK_a(\text{calcd}) + B$; Figure 3) with the pK_a scaling factors (see Experimental Section) $A = 0.2623$ (std. err. 0.0120) and $B = 2.5683$ (std. err. 0.2534) and the max absolute error of $0.28 pK_a$ units (abs errors 0.04, -0.17 , -0.05 , 0.28 , 0.01 , -0.11 for the azetidine-T (N^3 and N_{aza}), aza-ENA-T (N^3 and N_{aza}), 2'-amino-LNA-T (N^3 and N_{amino}), respectively).

These new correlation coefficients have been able to reproduce the experimental pK_a s of nucleobases (derived from NMR titrations) as well as the pK_a s of the endocyclic 2'-amino groups with abs. error of $<0.2 pK_a$ units (Table 3). It is noteworthy that the correlation coefficients derived in the earlier work⁵¹ have been underestimating the pK_a s of the endocyclic 2'-amino groups by $\sim 2 pK_a$ units compared to the experimental values (Table 3, pK_a values in parentheses).

Increase of the size of basis set and of the correlation level to B3LYP/6-31++G** has improved the overall correlation between theoretical and experimental pK_a s resulting in scaling factors $A = 0.4995$ (std. err. 0.0475) and $B = 1.4505$ (std. err. 0.6274), which however are still far away from those in the ideal combination of $A = 1$ and $B = 0$. The drastic change of the correlation coefficients which is found depending on the size of the basis set and the level of simulations, demonstrates the deficiencies of the adopted correlation scheme employing pK_a scaling factors (see Experimental Section for details) and highlights the need to exercise caution in its application.

Conclusions

(1) Comparison of the 1',2'- and 2',4'- conformationally constrained nucleosides show that despite the overall chemical similarity of the *North*-type sugar conformational constraints imposed by the respective modifications, the actual internal dynamics and conformational hyperspace are distinctively

different and indeed are very specific within these two groups of modified nucleosides.

(2) The 1',2'- versus 2',4'-constrained nucleosides share within the respective group not only intrinsic properties of the modified sugar moiety (preferred sugar pucker) but also molecular properties of the aglycon reflected in specific glycoside (χ) and the backbone torsions (γ and δ) as well as in distinctive dynamics pattern. All available data indicate that the 1',2'-fused conformational constraints give to the nucleoside more flexibility than that of the 2',4'-fused conformational constraints (Table 2, Figure S11 in SI).

(3) High amplitude and range of dynamics of the important backbone torsion δ indicate that 1',2'-fused nucleosides have higher flexibility of the backbone compared to the 2',4'-fused counterparts which is an important property to engineer in the oligonucleotides in order to exploit their physicochemical properties for the conformational control of duplex and/or triplex formation, or to achieve specific interaction of a modified ON with enzymes or other ligands. Thus, the replacement of the 2'-*O*- by the 2'-*N*- atom in the ENA and LNA analogues is found to influence profoundly the backbone tuning torsion γ to unusual *trans* conformation (Table 2, Figure S11 in SI) which potentially can lead to backbone transition⁵² into noncanonical α/γ substate.

(4) The two types of conformational characteristics in the *North*-constrained nucleoside blocks can be correlated with the footprints produced by the RNase H cleavage reaction of the heteroduplexes:^{1,11,20,56} (i) 1',2'-fused nucleosides with less rigid and *North-East*-type constraint ($P = 37^\circ \pm 27^\circ$, $\phi_m = 25^\circ \pm 18^\circ$), such as oxetane-T and azetidine-T blocks, showed poorer affinity to the target RNA compared to that of the native counterpart and produce local RNA–RNA mimics (hence, not cleaved by RNase H) resulting in a gap of the cleavage pattern of only five nucleotides in the ON/RNA duplexes.^{10,11,20,56,57} On the other hand, a more rigid pure *North*-type 2',4'-fused sugar constrained ENA- and LNA-types as well as their 2'-*N* analogues ($P = 19^\circ \pm 8^\circ$, $\phi_m = 48^\circ \pm 4^\circ$) introduced into ON showed a higher affinity to the target RNA; this transformed the local structure more RNA–RNA type and hence showed a stronger resistance to RNase H cleavage, exhibiting 6–8 nucleotide gaps.^{4,8}

(5) It has been found that the basicity of the endocyclic 2'-amino group in all furanose fused conformationally constrained nucleosides is both site- and ring-size dependent, which has distinct influence on the basicity of N^3 of the constituent 1-thymine moiety. Thus, the chemical nature of the conformational constraints in the sugar moiety can remarkably steer the physicochemical property, such as the pK_a of the constituent 1-thymine moiety, which, along with other factors^{55,58} can play a vital role in tuning the strength of the basepairing.

Experimental Section

A. Ab Initio and MD Calculations. Compounds **A–F** (Figure 1) have been simulated to investigate intrinsic dynamics and to build up their molecular structures using the following protocol: (i) Acquire 6-31G** Hartree–Fock optimized ab initio gas-phase

(55) Acharya, P.; Cheruku, P.; Chatterjee, S.; Acharya, S.; Chattopadhyaya, J. *J. Am. Chem. Soc.* **2004**, *126*, 2862–2869.

(56) Pradeepkumar, P. I.; Chattopadhyaya, J. *J. Chem. Soc., Perkin Trans.* **2001**, *2*, 2074–2083.

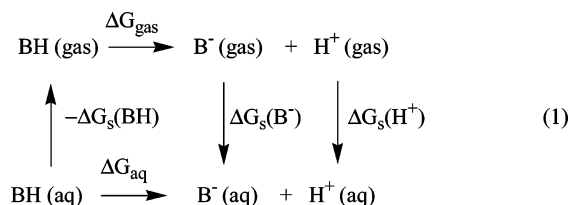
(57) Pradeepkumar, P. I.; Zamaratski, E.; Földesi, A.; Chattopadhyaya, J. *Tetrahedron Lett.* **2000**, *41*, 8601–8607.

(58) Shan, S.-O.; Herschlag, D. *Proc. Natl. Acad. Sci. U.S.A.* **1996**, *93*, 14474–14479.

(54) Koike, H.; Kimura, T.; Kawasaki, T.; Sada, T.; Ikeda, T.; Sanbuissho, A.; Saito, H. *Annu. Rep. Sankyo Res. Lab.* **2002**, *54*, 1–64.

geometries and atomic charges to derive force field parameters for MD; (ii) refine the Karplus parameters with the help of the NMR-derived and ab initio derived torsions; (iii) analyze the full conformational hyperspace using 2 ns MD simulations of the compounds **A–F** (Figure 1); (iv) derive initial dihedral angles from the observed $^3J_{\text{HH}}$ using Haasnoot–de Leeuw–Altona generalized Karplus equation;^{44,45} (v) perform NMR constrained molecular dynamics (MD) simulation (0.5 ns, 10 steps) simulated annealing (SA) followed by 0.5 ns NMR constrained simulations at 298 K using the NMR derived torsional constraints from step iv to yield NMR defined molecular structures of the compounds in question. The geometry optimizations of the modified nucleosides have been carried out by GAUSSIAN98 program package⁴⁶ at the Hartree–Fock level using 6-31G** basis set as well as employing Becke three-parameter (exchange) Lee, Yang, and Parr (B3LYP) correlation density functional theory (DFT) and 6-31++G** basis set. The atomic charges and optimized geometries from HF/6-31G** simulations of compounds **A–F** (Figure 1) have been used as AMBER⁴⁷ force field parameters employed in the MD simulations. The protocol of the MD simulations is based on Cheatham–Kollman’s⁵⁹ procedure employing a modified version of Amber 1994 force field as it is implemented in AMBER 7 program package.⁴⁷ Periodic boxes containing 707, 1125, 715, 715, 717, and 716 TIP3P⁴⁸ water molecules to model explicit solvent around azetidine-T, oxetane-T, aza-ENA-T, ENA-T, LNA-T, and 2'-amino-LNA-T nucleosides, respectively, were generated using xleap extending 12.0 Å from these molecules in three dimensions in both the NMR constrained and unconstrained MD simulations. SA protocol included 10 repeats of 25 ps heating steps from 298 to 400 K followed by fast 25 ps cooling steps from 400 to 298 K. During these SA and NMR constrained MD simulations, torsional constraints of 50 kcal mol⁻¹ rad⁻² were applied. The constraints were derived from the experimental $^3J_{\text{H1',H2'}}$, $^3J_{\text{H2',H3'}}$, and available $^3J_{\text{H7a/H7b,NH}}$ coupling constants using Haasnoot–de Leeuw–Altona generalized Karplus equation^{44,45} and parameters discussed in the text. Ten SA repeats were followed by a 0.5 ns MD run at constant 298 K temperature applying the same NMR constraints.

B. Method of pK_a Calculations. To predict pK_a values of the LNA-T, ENA-T, their nitrogen-containing analogues, as well as of the azetidine- and oxetane-fused T reported earlier⁵¹ we have carried out ab initio calculations utilizing (1) closed shell Hartree–Fock (HF) method employing 6-31G** basis set and (2) B3LYP correlation DFT employing the 6-31++G** basis set to calculate pK_a values from the traditional thermodynamics cycle (1).



Molecular geometries of all protonated and deprotonated nucleosides have been optimized in gas phase, and the effect of solvation has been estimated using Baron and Cossi’s implementation of the polarizable conductor CPCM model⁶⁰ in GAUSSIAN98⁴⁶ program package. Intrinsically this direct approach presents a considerable challenge to make an accurate prediction of absolute pK_a values due to manifestation of relatively small errors in the gas-phase thermodynamics and the solvation energy calculations as large errors in absolute pK_a values. For example, an error of 1.36 kcal/mol in the total free Gibbs energy results in error of 1 pK_a unit (for

discussion, see Liptak and Shields^{61,62} and references therein). We have therefore adopted an empirical correction scheme similar to that of Klicic and co-workers⁶³ and used by us earlier⁵¹ employing a set of 24 compounds altogether in the dataset (A, G, C, T, U native nucleobases and deoxy-A,G,C,T and ribo-A,G,C,U nucleosides), to compensate for deficiencies in both HF/6-31G** ab initio and solvation models with reasonably good correlation (with errors of up to 0.5 pK_a unit) to experimental pK_a values via the following correction scheme: pK_a (scaled) = A × pK_a (calcd) + B. Values of ΔG_s(H⁺) and ΔG(H⁺) were set to −262.5 kcal/mol⁶⁴ and −6.28 kcal/mol^{65,66} to be consistent with the analysis performed in ref 51.

C. pH-Dependent ¹H NMR Measurement. All NMR experiments were performed using Bruker DRX-500 and DRX-600 spectrometers. The 1 mM NMR samples of the 2'-amino-T (2'-amino-2'-deoxyribothymidine), 1',2'-azetidine-T (**A**), aza-ENA-T (**C**), and 2'-amino-LNA-T (**E**) in Figure 1 were prepared in D₂O solution with δ_{DSS} = 0.015 ppm as internal standard. All pH-dependent NMR measurements have been performed at 298 K. The pH values [with the correction of deuterium effect] correspond to the reading on a pH meter equipped with a calomel microelectrode (in order to measure the pH inside the NMR tube) calibrated with standard buffer solutions (in H₂O) of pH 4, 7 and 10. The pD of the sample has been adjusted by simple addition of microliter volumes of NaOD solutions (0.5, 0.1, and 0.01 M). The pH values are obtained by the subtraction of 0.4 from corresponding pD values [pH = pD − 0.4]. All ¹H spectra have been recorded using 128 K data points and 64 scans.

D. pH Titration of Aromatic Protons and pK_a Determination from Hill Plot Analysis. The pH titration studies were done over the range of pH (1.8 < pH < 12.2), with [0.2 – 0.3] pH interval for four 2'-amino-containing nucleosides: the 2'-amino-T, 1',2'-azetidine-T (**A**), aza-ENA-T (**C**), and 2'-amino-LNA-T (**E**). All pH titration studies consist of ~20 – 30 data points and the corresponding sigmoidal pH metric titration curves (Figures S1–S8 in SI) to determine the 2'-amino group protonation pK_a as well as the pK_a of N³(T) deprotonation (see Figure 9a,b in SI). The pH-dependent [over the range of pH 1.8 < pH < 12.2, with an interval of pH 0.2 – 0.3] ¹H chemical shifts (δ, with error ± 0.001 ppm) for all compounds have shown a sigmoidal behavior. Values of the pK_as have been determined from the inflection points of the NMR titration curves as well as based also on the Hill plot analysis using the following equation: pH = log((1 – α)/α) + pK_a, where α represents a fraction of the protonated species. The value of α has been calculated from the change of chemical shift relative to the deprotonated (D) state at a given pH (Δ_D = δ_D – δ_{obs}, for deprotonation, where δ_{obs} is the experimental chemical shift at a particular pH), divided by the total change in chemical shift between neutral (N) and deprotonated (D) state (Δ_T). So the Henderson–Hasselbach type equation can then be written as pH = log [(Δ_T – Δ_D)/Δ_D] + pK_a, and the pK_a is calculated from the linear regression analysis of the Hill plot.

Acknowledgment. Generous financial support from the Swedish Natural Science Research Council (Vetenskapsrådet), the Swedish Foundation for Strategic Research (Stiftelsen för Strategisk Forskning), and the EU-FP6 funded RIGHT project

(61) Liptak, M. D.; Shields, G. C. *J. Am. Chem. Soc.* **2001**, *123*, 7314–7319.

(62) Liptak, M. D.; Shields, G. C. *Int. J. Quantum Chem.* **2001**, *85*, 727–741.

(63) Klicic, J. J.; Friesner, R. A.; Liu, S. Y.; Guida, W. C. *J. Phys. Chem. A* **2002**, *106*, 1327–1335.

(64) Tawa, G. J.; Topol, I. A.; Burt, S. K.; Caldwell, R. A.; Rashin, A. A. *J. Chem. Phys.* **1998**, *109* (12), 4852–4863.

(65) Topol, I. A.; Tawa, G. J.; Burt, S. K.; Rashin, A. A. *J. Phys. Chem. A* **1997**, *101*, 10075–10081.

(66) Topol, I. A.; Tawa, G. J.; Caldwell, R. A.; Eissenstat, M. A.; Burt, S. K. *J. Phys. Chem. A* **2000**, *104*, 9619–9624.

(59) Cheatham, T. E., III; Kollman, P. A. *J. Am. Chem. Soc.* **1997**, *119*, 4805–4825.

(60) Barone, V.; Cossi, M. *J. Phys. Chem. A* **1998**, *102* (11), 1995–2001.

(Project no. LSHB-CT-2004-005276) to J.C. is gratefully acknowledged.

Supporting Information Available: The stack plots of the pH-dependent ^1H NMR chemical shifts of sugar and aromatic protons for compounds **A–F** (Figure 1) at 298 K (Figures S1–S7). Full records of references 45 and 46. NMR titration plots of pH vs chemical shift of specified marker proton to obtain $\text{p}K_{\text{a}}$ of 2'-amine protonation and $\text{p}K_{\text{a}}$ of N^3 deprotonations in 1',2'-azetidine-T, aza-ENA-T, 2'-amino-LNA-T, and 2'-amino-T as well as the results of respective Hill plot analysis (panels e–h, pH vs $\log[(\Delta_{\text{T}} - \Delta)/$

$\Delta]$) (Figures S8a,S8b). Frontier orbitals of the compounds **A–F** in Figure 1 (Table S1). IUPAC definition of sugar and backbone torsion angles as well as a section of a polynucleotide backbone showing the atomic numbering and notation for torsion angles (Figure S10). Dynamics of backbone (γ , δ) and glycoside bond (χ) torsions (deg) (Figure S11). Parameters of the MD simulations (Tables S2–S3). This material is available free of charge via the Internet at <http://pubs.acs.org>.

JO070356U